

# Supporting Information

## Probing Phonon Dynamics in Individual Single-Walled Carbon Nanotubes

Tao Jiang,<sup>†,⊥</sup> Hao Hong,<sup>‡,⊥</sup> Can Liu,<sup>‡</sup> Wei-Tao Liu,<sup>†,§</sup> Kaihui Liu,<sup>\*,‡</sup> and Shiwei Wu<sup>\*,†,§</sup>

<sup>†</sup> State Key Laboratory of Surface Physics, Key Laboratory of Micro and Nano Photonic Structures, and Department of Physics, Fudan University, Shanghai 200433, China

<sup>‡</sup> State Key Laboratory for Mesoscopic Physics, Collaborative Innovation Center of Quantum Matter, and School of Physics, Peking University, Beijing 100871, China

<sup>§</sup> Collaborative Innovation Center of Advanced Microstructures, Nanjing 210093, China

\*Corresponding emails: [swwu@fudan.edu.cn](mailto:swwu@fudan.edu.cn); [khliu@pku.edu.cn](mailto:khliu@pku.edu.cn)

<sup>⊥</sup> These authors contributed equally to this work.

**The Supporting Information includes:**

- 1. CVD growth of SWNTs**
- 2. Electron diffraction and optical spectroscopic measurements**
- 3. Time-resolved ASR spectroscopy**
- 4. Fitting procedure for extracting the phonon lifetime**

**Figure S1: Phonon lifetime as a function of chiral angle**

**Figure S2: Schematic of experimental setup**

**Table S1: Information for 14 SWNTs studied**

## **1. CVD growth of SWNTs**

In our experiments, suspended long single-walled carbon nanotubes were grown by CVD method across open slit structures ( $30 \times 500 \mu\text{m}$ ) fabricated on  $\text{SiO}_2/\text{Si}$  substrates. Typically, in the CVD growth we used methane in hydrogen ( $\text{CH}_4:\text{H}_2=1:2$ ) as gas feedstock and a thin film (0.1 nm) of iron as the catalyst. This suspended carbon nanotube is extremely clean and free of environmental effects, allowing us to explore the intrinsic physical properties of carbon nanotubes.<sup>1</sup>

## **2. Electron diffraction and optical spectroscopic measurements**

To get the structural and electronic properties, we combined electron diffraction and Rayleigh scattering/absorption techniques on the same carbon nanotubes. The electron diffraction patterns were detected by using nanofocused 80 keV electron beams in a JEOL 2010F TEM. Then from the diffraction pattern we can get the chirality (n,m) of nanotubes.<sup>2-4</sup> Rayleigh scattering and absorption spectra were applied to the suspended SWNTs to probe their electronic properties with a supercontinuum light source.<sup>5,6</sup>

## **3. Time-resolved ASR spectroscopy**

To perform the time-resolved ASR spectroscopy, two different colour laser beams were sent collinearly through a microscope objective (Nikon, 50X/NA0.45) onto the individual SWNTs. The laser polarization was parallel to the SWNT axis to obtain stronger excitation and detection signals. A pump beam (about 300-600  $\mu\text{W}$ ) at 820 nm from a 80 MHz femtosecond Ti:Sapphire oscillator (Spectra-Physics, MaiTai HP) was used to excite electron-hole pairs, which rapidly creates a high density of optical phonons via carrier-phonon relaxation. A delayed probe beam with weaker power (about 40-80

$\mu\text{W}$ ) from a synchronously pumped optical parametric oscillator (Spectra-Physics, Inspire), whose wavelength was tuned to match the nanotube optical resonance, was used to probe the hot phonon population by monitoring the G-mode ASR intensity.<sup>7,8</sup> Time-zero between the pump and probe beams was determined by the maximum four-wave mixing signal emitted from the silicon substrates. Emitted ASR signal in the back scattered direction was collected by the same objective and analysed by a liquid nitrogen cooled silicon CCD detector after passing through a spectrograph with appropriate filters (Princeton Instruments, Spec-10:100BR/LN\_eXcelon). The setup schematic is shown in Figure S2.

#### **4. Fitting procedure for extracting the phonon lifetime**

To extract the G-mode phonon lifetime, we followed the same methods as described in Ref. 7. One simple method was to fit the relaxation section of phonon dynamic curve with a single exponential decay, after the non-zero constant ASR intensity arising from the hot phonons created by the probe beam was deducted. The decay time constant is the G-mode phonon lifetime. The whole G-mode phonon dynamic curve could be also modelled as an abrupt rise at a delay time  $t_0$  ( $\sim 200$  fs) followed by an exponential decay with a time constant  $T_1$  (phonon lifetime). The experimental data were fitted by convoluting the intrinsic phonon dynamics with the finite duration of pump/probe pulses ( $\sim 170$  fs). The two different method yielded consistent value of phonon lifetime for a given set of data.

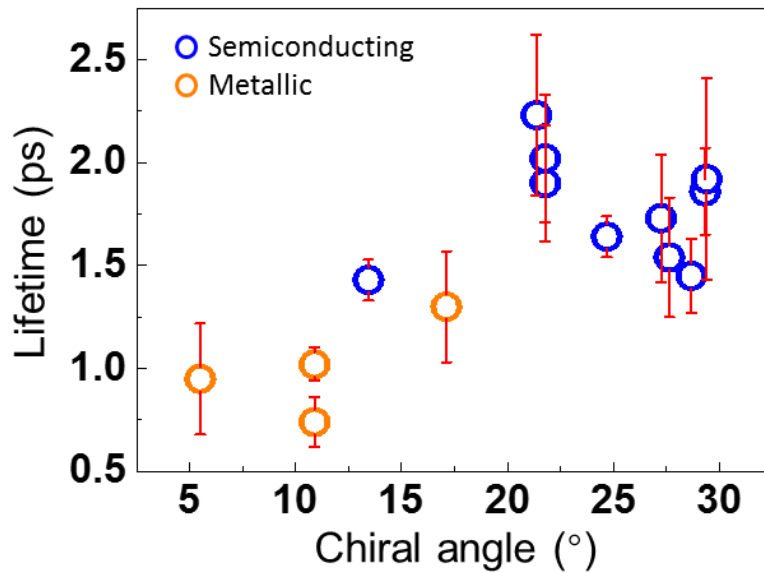


**Figure S1.** Phonon lifetime as a function of chiral angle. With chiral angle increases, the lifetime of metallic SWNT increases correspondingly, while the lifetime of semiconducting SWNT remains constant.

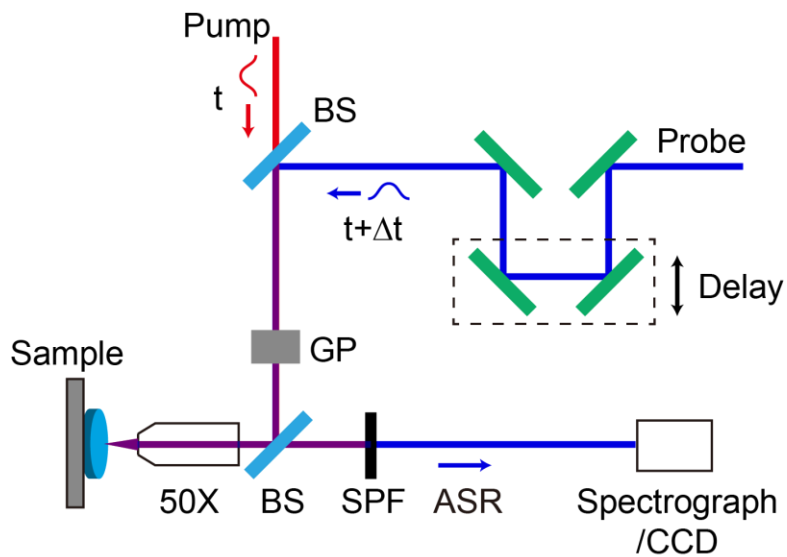


**Figure S2.** Schematic of experimental setup. BS: beam splitter, GP: Glan-Laser polarizer, SPF: short-pass filters, ASR: anti-Stokes Raman.

(n,m)	Mod (n-m,3)	Diameter (nm)	Chiral angle (°)	Phonon lifetime (ps)	Resonant energy (eV)
(35,21)	2	3.84	21.8	2.02 ± 0.31	S <sub>44</sub> =1.28, S <sub>55</sub> =1.77, <b>S<sub>66</sub>=1.89</b> , S <sub>77</sub> =2.42
(35,21)	2	3.84	21.8	1.90 ± 0.28	S <sub>44</sub> =1.28, S <sub>55</sub> =1.77, <b>S<sub>66</sub>=1.90</b> , S <sub>77</sub> =2.42
(25,8)	2	2.34	13.4	1.43 ± 0.10	S <sub>33</sub> =1.69, <b>S<sub>44</sub>=1.87</b>
(18,13)	2	2.11	24.6	1.64 ± 0.10	S <sub>33</sub> =1.74, <b>S<sub>44</sub>=2.07</b>
(15,13)	2	1.90	27.6	1.54 ± 0.29	<b>S<sub>33</sub>=1.92</b> , S <sub>44</sub> =2.26
(28,27)	1	3.73	29.4	1.92 ± 0.49	S <sub>55</sub> =1.79, S <sub>66</sub> =2.02, <b>S<sub>77</sub>=2.43</b>
(25,24)	1	3.32	29.3	1.86 ± 0.21	S <sub>44</sub> =1.46, <b>S<sub>55</sub>=1.95</b> , S <sub>66</sub> =2.18
(26,22)	1	3.26	27.2	1.73 ± 0.31	S <sub>33</sub> =1.46, <b>S<sub>44</sub>=1.98</b> , S <sub>55</sub> =2.22, S <sub>66</sub> =2.63
(24,14)	1	2.61	21.4	2.23 ± 0.39	S <sub>33</sub> =1.43, S <sub>44</sub> =1.79, <b>S<sub>55</sub>=2.33</b>
(13,12)	1	1.70	28.7	1.45 ± 0.18	<b>S<sub>33</sub>=2.07</b> , S <sub>44</sub> =2.51
(37,16)	0	3.69	17.1	1.30 ± 0.27	M <sub>22</sub> =1.53, M <sub>22</sub> =1.62, <b>M<sub>33</sub>=2.15</b> , M <sub>33</sub> =2.34
(32,8)	0	2.87	10.9	1.02 ± 0.08	M <sub>22</sub> =1.82, M <sub>22</sub> =2.03, <b>M<sub>33</sub>=2.51</b>
(34,4)	0	2.83	5.5	0.95 ± 0.27	M <sub>22</sub> =1.84, M <sub>22</sub> =2.06, <b>M<sub>33</sub>=2.50</b> , M <sub>33</sub> =2.91
(28,7)	0	2.51	10.9	0.74 ± 0.12	M <sub>22</sub> =2.01, <b>M<sub>22</sub>=2.28</b>

**Table S1.** Information for 14 SWNTs studied. The wavelength of the probe beam in time-resolved ASR spectroscopy was tuned to match the nanotube optical resonance,

which are labelled in bold in Table S1 for each SWNT.

### Supplementary References

(1) Liu, K. H.; Wang, W. L.; Wu, M. H.; Xiao, F. J.; Hong, X. P.; Aloni, S.; Bai, X. D.; Wang, E. G.; Wang, F. *Phys. Rev. B* **2011**, *83*, 113404.

(2) Wang, Z. L.; Poncharal, P.; de Heer, W. A. *Journal of Physics and Chemistry of Solids* **2000**, *61*, 1025-1030.

(3) Liu, Z. J.; Qin, L. C. *Chem. Phys. Lett.* **2005**, *408*, 75-79..

(4) Liu, K. H.; Xu, Z.; Wang, W. L.; Gao, P.; Fu, W. Y.; Bai, X. D.; Wang, E. G. *J. Phys. D* **2009**, *42*, 125412.

(5) Liu, K. H.; Deslippe, J.; Xiao, F.; Capaz, R. B.; Hong, X.; Aloni, S.; Zettl, A.; Wang, W.; Bai, X. D.; Louie, S. G.; Wang, E. G.; Wang, F. *Nat. Nanotechnol.* **2012**, *7*, 325-329.

(6) Liu, K. H.; Hong, X. P.; Choi, S.; Jin, C.; Capaz, R. B.; Kim, J.; Wang, W.; Bai, X.; Louie, S. G.; Wang, E. G.; Wang, F. *Proc. Natl. Acad. Sci. U. S. A.* **2014**, *111*, 7564-7569.

(7) Wu, S. W.; Liu, W.-T.; Liang, X. G.; Schuck, P. J.; Wang, F.; Shen, Y. R.; Salmeron, M. *Nano Lett.* **2012**, *12*, 5495-5499.

(8) Shah, J. *Ultrafast Spectroscopy of Semiconductors and Semiconductor Nanostructures*; Springer: Berlin, 1996.